High fidelity computation of electromagnetic resonant modes in cavities

M. Dawson, R. Sevilla, O. Hassan and K. Morgan

Zienkiewicz Centre for Computational Engineering, College of Engineering, Swansea University, UK SA1 8EN

{743587,R.Sevilla,O.Hassan,K.Morgan}@swansea.ac.uk

ABSTRACT

We present a method of obtaining properties of electromagnetic cavities with frequency dependent materials, such as the resonant frequencies, quality factors and mode shapes, using a high-order discontinuous Galerkin (DG) time-domain solver. Optimal convergence in the resonant frequency has been achieved for all numerical examples. The accuracy of resonant frequencies obtained is quantified and we present a study of errors due to geometrical approximation. Advantages of a multi-processor computation using Message Passing Interface (MPI) are demonstrated.

Key Words: *Discontinuous Galerkin; Electromagnetics; Resonant Cavities; Time Domain*

1. Introduction

Recent advances in manufacturing techniques, such as electron beam lithography make it possible to manufacture resonant cavities on the scale of the wavelength of light. These devices frequently have desirable qualities such as high quality factors and well defined resonant frequencies [1]. However, the typical scale and the geometric complexity introduce several challenges for numerical simulation.

The behaviour of these resonators is described by Maxwells' equations of classical electromagnetics. For dispersive materials, an auxiliary ordinary differential equation based on the Drude model of solids [2] is coupled to the Maxwell system. Frequency domain solvers are traditionally employed to find the resonant frequencies and associated modes, but as the scale and geometric complexity of the devices increase, the large eigenvalue system that must be solved becomes computationally prohibitive.

We propose using the Discontinuous Galerkin method with explicit time marching, which only requires solving a block diagonal system of equations for each timestep [3]. The frequency spectrum, resonant frequencies and quality factors are then recovered by a Fourier transform of the time domain solution.

2. DG solution of the transient Maxwell's equations in dispersive media

Maxwell's equations of classical electromagnetics and the auxiliary ordinary different equation required for dispersive media in linear, dimensionless, conservation form by

$$\frac{\partial \mathbf{U}}{\partial t} + \sum_{k=1}^{n_{sd}} \frac{\partial \mathbf{F}_k(\mathbf{U})}{\partial x_k} = \mathbf{S}(\mathbf{U}),\tag{1}$$

where n_{sd} denotes the number of spatial dimensions. The vector of unknowns, $\mathbf{U}$, is given by $\mathbf{U} = (\epsilon E_1, \epsilon E_2, \epsilon E_3, \mu H_1, \mu H_2, \mu H_3, J_1, J_2, J_3)^T$, the flux vectors, $\mathbf{F}_k$, are given by $\mathbf{F}_1 = (0, H_3, -H_2, 0, -E_3, E_2, 0, 0, 0)^T$, $\mathbf{F}_2 = (-H_3, 0, H_1, E_3, 0, -E_1, 0, 0, 0)^T$ and $\mathbf{F}_3 = (H_2, -H_1, 0, -E_2, E_1, 0, 0, 0, 0)^T$ and the source term, $\mathbf{S}$, is given by $\mathbf{S} = (0, 0, 0, 0, 0, 0, \omega_d^2 E_1 - \gamma_d J_1, \omega_d^2 E_2 - \gamma_d J_2, \omega_d^2 E_3 - \gamma_d J_3)^T$. Here $\mathbf{E} = (E_1, E_2, E_3)$ is the electric field intensity, $\mathbf{H} = (H_1, H_2, H_2)$ is the magnetic field intensity and $\mathbf{J} = (J_1, J_2, J_3)$ is the polarisation current. The material parameters ϵ, μ, ω and γ are the electric permittivity, magnetic permeability, plasma frequency and electron damping coefficient respectively.

We discretise the computational domain Ω on an unstructured mesh. The DG weak formulation [4] of (1) on an element Ω_e can then be written as

$$\int_{\Omega_e} \mathbf{W} \cdot \frac{\partial \mathbf{U}_e}{\partial t} d\Omega + \int_{\Omega_e} \mathbf{W} \cdot \left(\sum_{k=1}^{n_{sd}} \frac{\partial \mathbf{F}_k(\mathbf{U}_e)}{\partial x_k} - \mathbf{S}(\mathbf{U}_e) \right) d\Omega + \int_{\partial\Omega_e} \mathbf{W} \cdot \mathbf{A}_n^- [\![\mathbf{U}_e]\!] \, d\Gamma_e = 0 \,,$$

where $\mathbf{U}_e$ denotes the solution vector restricted to the element Ω_e, $\mathbf{W}$ is a vector of test functions and $[\![\mathbf{U}_e]\!] = \mathbf{U}_e - \mathbf{U}_{out}$ denotes the jump of the solution across the element boundary $\partial\Omega_e$. The boundary term, derived after introducing the numerical flux on the boundary and using a flux-splitting technique, results in

$$\mathbf{A}_n^- [\![\mathbf{U}_e]\!] = \frac{1}{2} \begin{pmatrix} -\mathbf{n} \times [\![\mathbf{H}]\!] + \mathbf{n} \times (\mathbf{n} \times [\![\mathbf{E}]\!]) \\ \mathbf{n} \times [\![\mathbf{E}]\!] + \mathbf{n} \times (\mathbf{n} \times [\![\mathbf{H}]\!]) \\ \mathbf{0}_{3x1} \end{pmatrix} \,,$$

where $\mathbf{n}$ is the outward unit normal of the element and $\mathbf{0}_{3x1}$ is a zero vector of dimension 3. After introducing the approximation of the solution and using a Galerkin formulation, the following system of ordinary differential equations is obtained

$$\mathbf{M}\frac{dU}{dt} + \mathbf{R}(U) = \mathbf{0} \,,$$

where U is the vector of nodal values, $\mathbf{M}$ is the block diagonal mass matrix and $\mathbf{R}(U)$ is the residual vector. The system of ordinary differential equations is advanced in time using a fourth-order explicit Runge-Kutta method.

3. Resonant frequencies and mode shapes

The engineering quantities of interest are the resonant frequencies and the associated modes shapes and quality factors. In order to obtain these quantities from time domain simulations, we begin with an intial field distribution containing a point excitation. Maxwells' equations are solved to advance the fields in time, and the amplitude of the solution field is recorded at fixed time intervals, Δt, at at least one point in space for a period of time, T. The resulting discrete field intensity signal is illustrated in Figure 1a. Taking the fast Fourier transform of the field intensity signal results in its frequency eigenspectrum, shown in Figure 1b for a 3-dimensional cubic cavity with a perfect electric conductory (PEC) boundary. The resonant frequencies of the cavity correspond to the locations of peaks in the spectrum, whilst the quality factors are related to peak widths. The mode shape associated to a given resonant frequency can be obtained as a postprocess, by taking the discrete Fourier transform at the desired frequency.

For a high fidelity computation of broadband spectrums, two properties of the fast Fourier transform must be taken into consideration: (1) the spectrum resolution is inversely proportional to T; (2) the highest resonant frequency that can be computed is inversely proportional to Δt. To alleviate the potentially large computational cost which results, we employ a high-order DG solver with a NEFEM [5] rationale. This enables the use of extremely coarse meshes that guarantee that the time step of the explicit time marching algorithm is not restricted by the stability condition, but by the maximum frequency that is to be resolved. In addition, an efficient parallel implementation using MPI has been developed, enabling to dramatically reduce the computational time required to advance the solution large periods of time.

4. Numerical Results

The solver was validated validated using a rectangular 2-dimensional cavity filled with a dispersive medium ($\epsilon_\infty = 1, \sigma = 1, \omega = 6.7433, \gamma = 0.0799$), surrounded by a perfect electric conductor, with a width twice its length. Figure 2a shows how error in the resonant frequency, calculated relative to a reference solution, converges with T to a final numerical error due to spatial discretisation. Optimal

(a) Signal obtained from simulation run.

(b) Eigenspectrum obtained by FFT
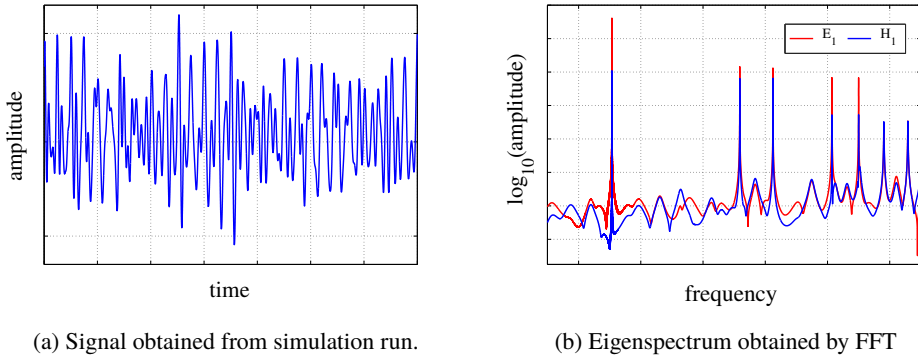
Figure 1: Signal and corresponding eigenspectrum obtained from a time domain simulation for a cubic, free-space cavity with a PEC boundary.

convergence of the error in resonant frequency is shown in Figure 2b, the error convergences as the numerical dispersion error, at a rate $h^{2(p+2)}$.

(a) Convergence of the error in calculated resonant frequency with T for three different meshes.

(b) h-convergence of the error in resonant frequency obtained for the fundamental frequency.
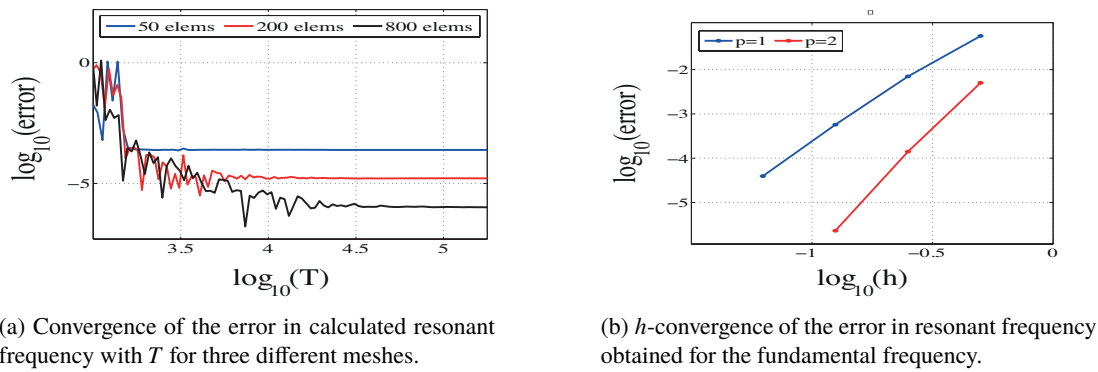
Figure 2: Results for a rectangular cavity filled with a dispersive medium, surrounded by a PEC boundary

A circular free-space cavity is used to illustrate the effect of boundary approximations on computed resonant frequencies. In Figure ??, convergence of error for p- and h-refinement is shown for iosparametric elements and NEFEM elements. The geometrical error can be seen to have a significant effect for low-order planar elements.

(a) Convergence of error in resonant frequency with square root of number of degrees of freedom for mode shown in (b).

(b) Meshes for resonant frequency error below 10^{-3}, left to right: planar isoparametric elements, $p = 1$ nefem elements, $p = 4$ isoparametric elements.
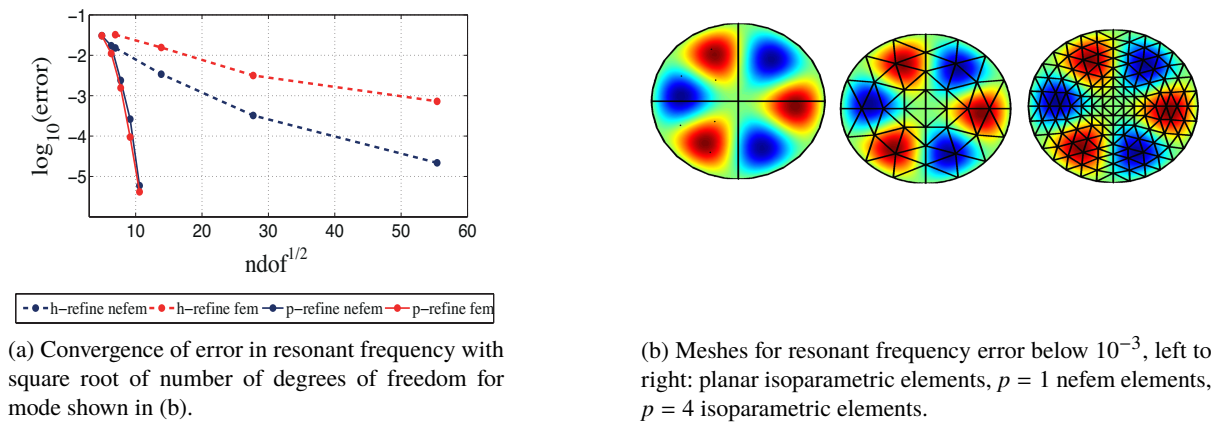
Figure 3: Results for a circular free-space cavity surrounded by a PEC boundary.
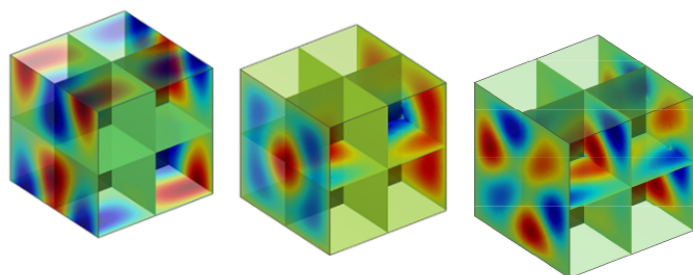
(a) Examples of mode shape obtained
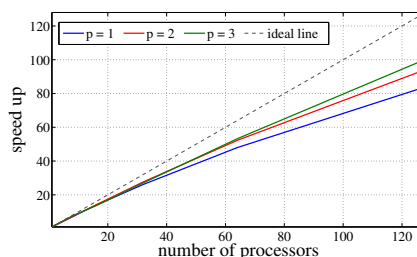
(b) Parallel speed up for a mesh of 12,288 planar hexahedral elements

Figure 4: Results for fully 3-dimensional cubic cavity with PEC boundaries

Parallel computation allows computation of resonant frequencies and mode shapes for challenging realistic 2- and 3-dimensional geometries with high accuracy, in a reasonable run time. Dramatic speed increases can be obtained for larger meshes, notable with higher-order elements, as illustrated by an almost linear speed up shown in Figure 4b.

5. Conclusions

A method has been presented for obtaining electromagnetic resonance properties of cavities using a parallelised discontinuous Galerkin time domain solver. We validated the method by showing *h*-convergence of the error in resonant frequencies. The method has been validated and optimal convergance rates in the resonant frequency error has been achieved. The effect of geometrical representation and high-order elements on resonant frequencies have been quantified and the advantages of parallelisation quantified.

Acknowledgements

References

[1] K. Busch, M. König, and J. Niegemann. Discontinuous Galerkin methods in nanophotonics. *Laser & Photonics Reviews*, 5(6):773–809, 2011.

[2] A. Taflove. *Computational Electrodynamics: The Finite-difference Time-domain Method*. Antennas and Propagation Library. Artech House, 1995.

[3] R. Sevilla, O. Hassan, and K. Morgan. The use of hybrid meshes to improve the efficiency of a discontinuous Galerkin method for the solution of Maxwells' equations. *Computers & Structures*, 137:2–13, 2014.

[4] J. Hesthaven and T. Warburton. *Nodal discontinuous Galerkin methods: algorithms, analysis, and applications*, volume 54. Springer Science & Business Media, 2007.

[5] R. Sevilla, S. Fernández-Méndez, and A. Huerta. Nurbs-enhanced finite element method (nefem). *International Journal for Numerical Methods in Engineering*, 76(1):56–83, 2008.